This article has been accepted for publication in a future issue of this journal, but has not been fully edited. Content may change prior to final publication. Citation information: DOI 10.1109/TVT.2014.2359233, IEEE Transactions on Vehicular Technology

On the Banded Approximation of the Channel Matrix for Mobile OFDM Systems

Ting-Li Liu[1], Wei-Ho Chung[2], Shih-Yi Yuan[3], Sy-Yen Kuo[1*]
Department of Electrical Engineering, National Taiwan University, Taipei, Taiwan[1]
Research Center for Information Technology Innovation, Academia Sinica, Taipei, Taiwan[2]
Department of Communications Engineering, Feng Chia University, Taichung, Taiwan[3]
E-mail:*sykuo@cc.ee.ntu.edu.tw

***Abstract*—In the mobile orthogonal frequency-division multiplexing (OFDM) systems, a frequency-domain channel matrix represents the same-carrier channel frequency response (CFR) in the diagonal and inter-carrier interference (ICI) between the subcarriers in the off-diagonals, respectively. A variety of the banded equalizers manipulated the banded approximation of the channel matrix to be exploited by the low-complexity equalizations. In this paper, we derive a simple and tight lower bound on the variance of the individual coefficients in the channel matrix for insights of the banded approximations. We obtain the errors introduced with the banded approximation and the ICI-mitigation gains of the banded equalizers in simple closed forms. The derivations of the banded approximation errors are beneficially applicable to the equalizers that perform the minimum mean square error (MMSE) estimation with the banded channel matrix. Simulations show that both the block MMSE banded equalizers and the block turbo MMSE banded equalizers significantly reduce the error floors by considering the banded approximation errors.**

***Index Terms*—Orthogonal frequency-division multiplexing (OFDM), inter-carrier interference (ICI), banded approximation.**

I. Introduction

Orthogonal frequency-division multiplexing (OFDM) is one of the effective transmission schemes and is widely used in many standards such as DVB-T/H, DAB, IEEE 802.11 and 802.16, etc. In a time-invariant frequency-selective channel, OFDM can eliminate inter-symbol interference (ISI) and render simple one-tap equalization for each subcarrier [1]. In a time-variant channel, the OFDM subcarriers are coupled with inter-carrier interference (ICI) since the orthogonality among OFDM subcarriers is destroyed by Doppler spreads. The one-tap equalization becomes suboptimal in Doppler-affected channels [2]. As a consequence, more powerful equalization with ICI suppression is required for mobile OFDM systems.

A variety of techniques have been proposed to counteract the ICI introduced with the Doppler spreads in mobile OFDM systems. Most of these techniques [3]–[20] employed a frequency-domain channel matrix $\mathbf{H}$ of a size of $N \times N$ to describe the interactions among N subcarriers. A diagonal entry in the channel matrix, denoted as $[\mathbf{H}]_{a,a}$, represents the channel frequency response (CFR) on ath subcarrier. In addition, an arbitrary off-diagonal entry, denoted as $[\mathbf{H}]_{a,b}$, records the ICI fraction which the signal for bth subcarrier imposes on ath subcarrier [21]. Although the channel matrix provides an explicit structure to interpret the CFRs and the ICI fractions distributed in N^2 pairs of the subcarriers, handling the channel matrix entails significant increase in complexity. Consequently, varieties of recent works [8]–[20] for the channel estimation and the equalization of mobile OFDM systems have been proposed to manipulate the channel matrix in linear complexity. These works often employed the banded approximation of the channel matrix.

The banded approximation of the channel matrix is based on the property where most ICI power spreads within a few adjacent subcarriers. Therefore, in the channel matrix, the entries corresponding to the ICI fractions relating two distant subcarriers are considered as insignificant and negligible. Considering the ICI power coming within Qth adjacent subcarriers, we manipulate a Qth banded approximation on the channel matrix. As a result, the channel matrix is approximated by the banded matrix that retains the coefficients in the $2Q+1$ central diagonals and sets the other coefficients to zeros.

Utilizing the banded approximations, the prior works reformulated the minimum mean square error (MMSE) block linear equalizer (BLE) [16]–[18] and the MMSE serial linear equalizer (SLE) [8], [15] to linear complexity $O(Q^2N)$ without significant impacts on bit error rate (BER) performance. With properly designed pilot clusters [22], the banded channel matrix can be efficiently estimated through the basis expansion model [12]. However, the practice of the banded approximation involves two major challenges: 1) the selection of the efficient band (Q) upon various factors such as the normalized maximum Doppler frequency, the subcarrier number, the propagation model and the techniques of detections, etc; 2) the analysis on the performance degradation by the banded approximation upon a selected band Q. To the best of the authors' knowledge, P. Schniter [15] attempts to deal with the 1st challenge and proposed $Q \geq \lceil f_D + 1 \rceil$ for Rayleigh fading channels, where f_D denotes the maximum Doppler frequency normalized to the subcarrier spacing. As to the 2nd challenge, a universal lower bound on the partial ICI was expressed in [8] to assess the errors introduced with the banded approximations.

The inequality $Q \geq \lceil f_D + 1 \rceil$ was first employed as a rule of thumb to determine the band Q in the prior works [11]–[13], [15]–[18]. This rule degrades to $Q \geq 2$ for $f_D \leq 100\%$ and

Acknowledgment: This research was supported by Ministry of Science and Technology, Taiwan under Grant NSC 102-2221-E-002-136-MY3.

This article has been accepted for publication in a future issue of this journal, but has not been fully edited. Content may change prior to final publication. Citation information: DOI 10.1109/TVT.2014.2359233, IEEE Transactions on Vehicular Technology

hence the prior works [15]–[18] selected the minimum $Q = 2$. However, the recent works in [11]–[13] called for larger bands to support lower BER performance as well as higher mobility. Therefore, the need for an updated evaluation on the banded approximation becomes apparent. In this paper, we seek to answer the challenges about the banded approximation. In [23], a pair of upper and lower bounds on the total ICI power for the OFDM systems in the specific time-varying channel models were derived to provide useful insights. Motivated by [8] and [23], we derive a simple lower bound on the variance of the individual coefficients in the channel matrix of the specific channel models in [23]. Accordingly, we provide insights into the banded structure of the channel matrices responding to different channel models. The lower bound of the banded approximation errors is derived in a simple closed form, which is tighter than the universal lower bound derived in [8].

The analysis of the banded approximation errors is beneficial for the prior techniques that employed the banded approximation. As a generalized application, we propose to take the banded approximation errors into account in the signal-to-interference-plus-noise ratio (SINR) of the MMSE estimation core of the banded equalizers in [8], [15]–[18]. With simulation results, we show that the simple lower bounds derived in this paper accurately predict the mean squares of the individual coefficients in the channel matrix and the sum of square errors introduced with the banded approximation, respectively. Employing the predictions of the banded approximation errors, we enhance the block MMSE banded equalizer [17] and the block turbo MMSE banded equalizer [18] with significantly lower error floors than those ignoring the banded approximation errors.

The rest of this paper is organized as follows. In section II, we derive the variances of the individual coefficients in the channel matrix for the systems in the channel models of interest. In section III, we discuss the banded approximations of the channel matrix with a simple lower bound of the errors, the ICI-mitigation gains of the banded equalizers and a generalized application for the banded MMSE equalizers. The simulation results are presented in section IV. In section V, we briefly conclude the methodology and findings presented in this paper.

Notation: We use upper (lower) boldface letters to denote matrices (column vectors). The $(\cdot)^H$ and $\|\cdot\|$ denote complex conjugate transpose and the Frobenius norm of a matrix, respectively. The $(\cdot)^*$ denotes complex conjugate. The $[\mathbf{A}]_{m,n}$ indicates the entry in the mth row and nth column of matrix $\mathbf{A}$. The $\mathbf{I}_n$ represents the $n \times n$ identity. The operator $\circ$ denotes element-wise product between two matrices. The $\delta(\cdot)$ denotes the Kronecker delta; the $\langle\cdot\rangle_N$ represents the modulo-N operation; the $E\{\cdot\}$ denotes the statistical expectation. The $*$ denotes convolution and $\mathcal{R}$ represents the set of real numbers.

II. The variance of the coefficients in channel matrix

A. Theoretical expressions

We consider the OFDM systems over the linear time-varying (LTV) channel, with N subcarriers and the cyclic prefix (CP) of length no less than the maximum channel delay spreads L. The LTV channel is modeled by $h_t(n,l)$, which denotes the channel impulse response of the lth tap at time n. Assuming perfect time synchronization, we express the output of discrete Fourier transform (DFT) unit $\mathbf{z} = [z_0, z_1, \cdots, z_{N-1}]^T$ after CP removal as

$$\mathbf{z} = \mathbf{H}\mathbf{x} + \mathbf{w} \tag{1}$$

where $\mathbf{H}$ denotes the $N \times N$ frequency-domain channel matrix of the coefficients previously derived in [20] as

$$[\mathbf{H}]_{a,b} = \frac{1}{N}\sum_{n=0}^{N-1}\sum_{l=0}^{L-1} h_t(n,l)\, e^{\frac{-j2\pi bl}{N}} e^{\frac{j2\pi(b-a)n}{N}}, \quad 0 \le a, b \le N-1. \tag{2}$$

The $\mathbf{x}$ represents the $N \times 1$ vector for the modulated symbol and $\mathbf{w}$ denotes the $N \times 1$ vector for frequency-domain Gaussian noise. In this paper, we consider the equalization individually in one symbol duration, and hence the symbol index is omitted for brevity.

Assuming the wide-sense stationary uncorrelated scattering (WSSUS) model for the LTV channels, we have

$$E\{h_t(n,l)\, h_t^*(n-q, l-r)\} = \gamma_t(q)\, {\sigma_t}^2(l)\, \delta(r) \tag{3}$$

where $\gamma_t(q)$ denotes the normalized tap autocorrelation and ${\sigma_t}^2(l)$ denotes the variance of the lth tap. Accordingly, the Doppler spectrum of the LTV channels can be expressed [15] as

$$S(\phi) \equiv \sum_q \gamma_t(q)\, e^{-j\phi q}, \ \phi \in \mathcal{R}, \tag{4}$$

where ϕ denotes the angular Doppler frequency in radians normalized to bandwidth. Letting $f = \frac{N}{2\pi}\phi$ be the Doppler frequency in Hz normalized to subcarrier spacing, we denote $s(f)$ as the Doppler spectrum defined in f. Subject to $\int_{-\phi_D}^{\phi_D} S(\phi)\, d\phi = \int_{-f_D}^{f_D} s(f)\, df = 1$ where ϕ_D and f_D denote the normalized maximum Doppler frequencies for ϕ and f, respectively, we obtain $s(f) = \frac{2\pi}{N} S(\phi)\big|_{\phi=\frac{2\pi f}{N}}$.

To analyze the interference between two subcarriers, we have a N based cyclic number p denoting the "Doppler index" previously defined in [15] to count the number of subcarriers from the sourcing subcarrier to the sinking subcarrier for the entries in the channel matrix. As a consequence, the Doppler index for an arbitrary entry $[\mathbf{H}]_{a,b}$ is given by $p \equiv \langle b-a \rangle_N$, $0 \le p \le N-1$. With the potential instability of frequency oscillators at both the transmitter and the receiver, we include the carrier frequency offset (CFO) in the system model. Assuming the invariance of CFO in an OFDM symbol duration, we utilize the derivation by P. Schniter in [15] to obtain the variance of the coefficients of the Doppler index p in the channel matrix as

$${\sigma_F}^2(p) = (S * V)(\phi)\Big|_{\phi=\frac{2\pi(p+f_O)}{N}} \cdot \sum_{l=0}^{L-1} {\sigma_t}^2(l), \tag{5}$$

where $S(\phi)$ is defined in (4), f_O denotes the CFO normalized to the subcarrier spacing, and $V(\phi)$ represents the Dirichlet

This article has been accepted for publication in a future issue of this journal, but has not been fully edited. Content may change prior to final publication. Citation information: DOI 10.1109/TVT.2014.2359233, IEEE Transactions on Vehicular Technology

function as

$$V(\phi) = \left(\frac{\sin \frac{\phi N}{2}}{N \sin \frac{\phi}{2}} \right)^2. \quad (6)$$

Without loss of generality, we normalize $\sum_{l=0}^{L-1} {\sigma_t}^2(l) = 1$. Inserting (6) into (5), we obtain

$${\sigma_F}^2(p) = \int_{-\phi_D}^{\phi_D} S(\phi) \left(\frac{\sin\left(\pi p + \pi f_O - \frac{N}{2}\phi\right)}{N \sin\left(\frac{\pi(p+f_O)}{N} - \frac{\phi}{2}\right)} \right)^2 d\phi. \quad (7)$$

Inserting $\sin^2\left(\pi p - \frac{N}{2}\phi\right) = \sin^2\left(\frac{N}{2}\phi\right)$, $S(\frac{2\pi f}{N}) = \frac{N}{2\pi} s(f)$ and $\phi = \frac{2\pi f}{N}$ into (7), we derive

$${\sigma_F}^2(p) = \int_{-f_D}^{f_D} s(f) \left(\frac{\sin(\pi f_O + \pi f)}{N \sin\left(\frac{\pi}{N}(p + f_O - f)\right)} \right)^2 df. \quad (8)$$

By (8), the Doppler spectrum and the CFO collectively determine the variances of the coefficients of the Doppler index p in the channel matrix. Since the CFO in the mobile OFDM systems can be well estimated and compensated [24], [25], we consider the perfect frequency synchronization, i.e., $f_O = 0$, in later discussions. Focusing on the broadband mobile OFDM systems, we assume in this paper that the systems have large subcarrier numbers, e.g., $N \geq 256$, satisfying the approximation $\sin(\frac{\pi f_D}{N}) = \frac{\pi f_D}{N}$, i.e., $\frac{\pi f_D}{N} \to 0$.

B. The upper bound and the lower bound

In this subsection, we input the statistics of the LTV channel to derive a pair of upper and lower bounds on the variances of the coefficients expressed in (8). Being a N-cyclic number, the Doppler index p is defined in the domain $0 \leq p \leq N-1$. For convenience to express the bounds, we alter the domain to $-\frac{N}{2}+1 \leq p \leq \frac{N}{2}$ and derive the bounds on ${\sigma_F}^2(p)$ for $p = 0$, $1 \leq p \leq \frac{N}{2}-1$, $-\frac{N}{2}+1 \leq p \leq -1$ and $p = \frac{N}{2}$, respectively.

First, we consider ${\sigma_F}^2(0)$ at the diagonal of the channel matrix. Inserting $p = 0$ into (8) and applying the approximation $N \sin(\frac{\pi f}{N}) = \pi f$, we obtain

$${\sigma_F}^2(0) = \int_{-f_D}^{f_D} s(f) \operatorname{sinc}^2(f)\, df \quad (9)$$

where the sinc function is defined as $\operatorname{sinc}(x) \equiv \sin(\pi x)/\pi x$.

By the Taylor series expansions of $\operatorname{sinc}^2(f)$ function at $f = 0$, a pair of upper and lower bounds are derived as

$$1 - \tfrac{1}{3}(\pi f)^2 \leq \operatorname{sinc}^2(f) \leq 1 - \tfrac{1}{3}(\pi f)^2 + \tfrac{2}{45}(\pi f)^4. \quad (10)$$

Inserting (10) into (9), we derive

$$1 - \tfrac{\alpha_1}{3}(\pi f_D)^2 \leq {\sigma_F}^2(0) \leq 1 - \tfrac{\alpha_1}{3}(\pi f_D)^2 + \tfrac{2\alpha_2}{45}(\pi f_D)^4 \quad (11)$$

where $\alpha_m = \frac{1}{{f_D}^{2m}} \int_{-f_D}^{f_D} f^{2m} s(f)\, df$, $m = 1, 2$ [23]. For the LTV channel models of interest, these constants previously derived in [23] are listed in Table I.

In the channel matrix, the diagonal entries determine the channel frequency response (CFR) and the off-diagonal elements account for ICI parts. Hence, we obtain the total ICI power $P_{ICI} = 1 - {\sigma_F}^2(0)$. According to (11), we derive

$$\tfrac{\alpha_1}{3}(\pi f_D)^2 - \tfrac{2\alpha_2}{45}(\pi f_D)^4 \leq P_{ICI} \leq \tfrac{\alpha_1}{3}(\pi f_D)^2 \quad (12)$$

that are exactly the same bounds on the total ICI power as previously derived in [23].

TABLE I. The α_1 and α_2 for the channel models of interest.

Models	Doppler spectrum $s(f)$	α_1	α_2
Two-path	$\frac{1}{2}\delta(f+f_D) + \frac{1}{2}\delta(f-f_D)$	1	1
Jakes	$\frac{1}{\pi f_D \sqrt{1-(f/f_D)^2}},\ \lvert f\rvert \leq f_D$	$\frac{1}{2}$	$\frac{3}{8}$
Uniform	$\frac{1}{2f_D},\ \lvert f\rvert \leq f_D$	$\frac{1}{3}$	$\frac{1}{5}$

Next, we consider ${\sigma_F}^2(p)$, $1 \leq p \leq \frac{N}{2}-1$ in (8) for the variance of the off-diagonal coefficients of the channel matrix. Utilizing the property that $\sin(x) > 0$ and $\sin(x)$ monotonically increases in $x \in (0, \pi/2)$, we derive

$$\begin{aligned} &\frac{1}{N^2 \sin^2\left(\frac{\pi}{N}(p+f_D)\right)} \leq \frac{1}{N^2 \sin^2\left(\frac{\pi}{N}(p-f)\right)} \\ &\leq \frac{1}{N^2 \sin^2\left(\frac{\pi}{N}(p-f_D)\right)},\ \lvert f\rvert \leq f_D,\ 1 \leq p \leq \tfrac{N}{2}-1. \end{aligned} \quad (13)$$

To examine the tightness of the bounds, we consider $N \to \infty$ and convert (13) into $(p+f_D)^{-2} \leq (p+f)^{-2} \leq (p-f_D)^{-2}$. Accordingly, the normalized difference from the upper bound to the lower bound can be approximated as $\frac{4f_D}{p}$. Hence, the larger p and the smaller f_D result in the tighter bounds in (13).

Inserting (13) into (8), we obtain

$$\begin{aligned} &\frac{\int_{-f_D}^{f_D} s(f) \sin^2(\pi f) df}{N^2 \sin^2\left(\frac{\pi}{N}(p+f_D)\right)} \leq {\sigma_F}^2(p) \\ &\leq \frac{\int_{-f_D}^{f_D} s(f) \sin^2(\pi f) df}{N^2 \sin^2\left(\frac{\pi}{N}(p-f_D)\right)},\ 1 \leq p \leq \tfrac{N}{2}-1. \end{aligned} \quad (14)$$

By the Taylor series expansion of $\sin^2(\pi f)$ function at $\pi f = 0$, a pair of upper and lower bounds on $\sin^2(\pi f)$ is derived as

$$(\pi f)^2 - \tfrac{1}{3}(\pi f)^4 \leq \sin^2(\pi f) \leq (\pi f)^2. \quad (15)$$

Inserting (15) into $\int_{-f_D}^{f_D} s(f) \sin^2(\pi f) df$, we derive

$$\begin{aligned} \alpha_1(\pi f_D)^2 - \frac{\alpha_2}{3}(\pi f_D)^4 &\leq \int_{-f_D}^{f_D} s(f) \sin^2(\pi f) df \\ &\leq \alpha_1 (\pi f_D)^2 \end{aligned} \quad (16)$$

where α_1 and α_2 are given in (11) and Table I.

Substituting the upper bound and the low bound in (16) for $\int_{-f_D}^{f_D} s(f) \sin^2(\pi f) df$ in (14), respectively, we obtain a pair of upper and lower bounds on the variance of the off-diagonal coefficients in the channel matrix as

$$\begin{aligned} &\frac{\alpha_1(\pi f_D)^2 - \frac{\alpha_2}{3}(\pi f_D)^4}{N^2 \sin^2\left(\frac{\pi}{N}(p+f_D)\right)} \leq {\sigma_F}^2(p) \\ &\leq \frac{\alpha_1(\pi f_D)^2}{N^2 \sin^2\left(\frac{\pi}{N}(p-f_D)\right)},\ 1 \leq p \leq \tfrac{N}{2}-1. \end{aligned} \quad (17)$$

With the higher order terms in the Taylor expansions, the lower bounds are closer to the exact evaluations than the upper

This article has been accepted for publication in a future issue of this journal, but has not been fully edited. Content may change prior to final publication. Citation information: DOI 10.1109/TVT.2014.2359233, IEEE Transactions on Vehicular Technology

bounds.

Third, we consider ${\sigma_F}^2(p)$ in $-\frac{N}{2}+1 \le p \le -1$ which is symmetric to those in $1 \le p \le \frac{N}{2}-1$. Hence, the bounds are simply inferred to as

$$\begin{aligned}\frac{\alpha_1(\pi f_D)^2 - \frac{\alpha_2}{3}(\pi f_D)^4}{N^2 \sin^2\left(\frac{\pi}{N}(p-f_D)\right)} &\le {\sigma_F}^2(p) \\ &\le \frac{\alpha_1(\pi f_D)^2}{N^2 \sin^2\left(\frac{\pi}{N}(p+f_D)\right)},\ -\tfrac{N}{2}+1 \le p \le -1.\end{aligned} \tag{18}$$

For the last term, we input $p = \frac{N}{2}$ to (8) and obtain

$${\sigma_F}^2\left(\frac{N}{2}\right) = \int_{-f_D}^{f_D} s(f)\left(\frac{\sin(\pi f)}{N\cos\frac{\pi f}{N}}\right)^2 df. \tag{19}$$

By using $\frac{\pi f_D}{N} \to 0$, we insert $\cos\frac{\pi f}{N} = 1$ into (19) and obtain ${\sigma_F}^2\left(\frac{N}{2}\right) = \frac{1}{N^2}\int_{-f_D}^{f_D} s(f)\sin^2(\pi f)df$. With the upper bound in (16), it turns out ${\sigma_F}^2\left(\frac{N}{2}\right) \le \alpha_1\left(\frac{\pi f_D}{N}\right)^2 \to 0$. As a consequence, we obtain the approximation ${\sigma_F}^2\left(\frac{N}{2}\right) = 0$.

C. The simple lower bound in symmetric Doppler spectrum

Assuming the channels of the Doppler spectrum are symmetric to the axis of zero frequency, e.g., those in Table I, we derive the simple lower bounds on the variance of the off-diagonal coefficients in the channel matrix. In this subsection, we consider ${\sigma_F}^2(p)$ in $1 \le p \le \frac{N}{2}-1$; then those in $\frac{N}{2}+1 \le p \le -1$ can be simply obtained by similar procedures.

With a symmetric Doppler spectra, we rewrite (8) as

$$\begin{aligned}{\sigma_F}^2(p) = \int_0^{f_D} s^\dagger(f)\frac{\sin^2(\pi f)}{N^2}\Bigg(&\sin^{-2}\left(\frac{\pi}{N}(p-f)\right) \\ &+\sin^{-2}\left(\frac{\pi}{N}(p+f)\right)\Bigg)df\end{aligned} \tag{20}$$

where $s^\dagger(f)$ determines a half of the Doppler spectrum in $f \ge 0$. In Appendix A, we prove $\sin^{-2}\left(\frac{\pi}{N}(p-f)\right) + \sin^{-2}\left(\frac{\pi}{N}(p+f)\right) \ge 2\sin^{-2}\left(\frac{\pi p}{N}\right)$ for $0 \le f \le f_D$ and $1 \le p \le \frac{N}{2}-1$. Hence, we obtain

$$\begin{aligned}{\sigma_F}^2(p) &\ge \frac{2\int_0^{f_D} s^\dagger(f)\sin^2(\pi f)df}{N^2\sin^2\left(\frac{\pi p}{N}\right)} \\ &= \frac{\int_{-f_D}^{f_D} s(f)\sin^2(\pi f)df}{N^2\sin^2\left(\frac{\pi p}{N}\right)},\ 1 \le p \le \tfrac{N}{2}-1.\end{aligned} \tag{21}$$

Substituting the lower bound derived in (16) for $\int_{-f_D}^{f_D} s(f)\sin^2(\pi f)df$ in (21), we derive a low bound on ${\sigma_F}^2(p)$ as

$${\sigma_F}^2(p) \ge \frac{\alpha_1(\pi f_D)^2 - \frac{\alpha_2}{3}(\pi f_D)^4}{N^2\sin^2\left(\frac{\pi p}{N}\right)},\ 1 \le p \le \tfrac{N}{2}-1. \tag{22}$$

Inserting $1/\left(N^2\sin^2(\frac{\pi p}{N})\right) \ge 1/(\pi p)^2,\ 1 \le p \le \frac{N}{2}-1$ into (22), we obtain the simple lower bound as

$${\sigma_F}^2(p) \ge \frac{1}{p^2}\left(\alpha_1 {f_D}^2 - \frac{\alpha_2}{3}\pi^2 {f_D}^4\right),\ 1 \le p \le \tfrac{N}{2}-1. \tag{23}$$

In Appendix B, we further derived $\varepsilon_F(p) = \frac{3\alpha_2 {f_D}^4}{p^4}$ for the errors between the variance of the off-diagonal coefficients and its simple lower bound in (23) based on the approximations of the 4th-order Taylor expansions. In Appendix C, we further improve (23) by using the approximations of the 8th-order Taylor expansions for the scenarios with relatively high Doppler frequencies. Using the simple lower bound in (23) as an approximation of ${\sigma_F}^2(p)$, we show that the variances of the off-diagonal coefficients in the channel matrix decrease with $1/p^2$ [2] and are independent to the subcarrier number (N) of the OFDM systems.

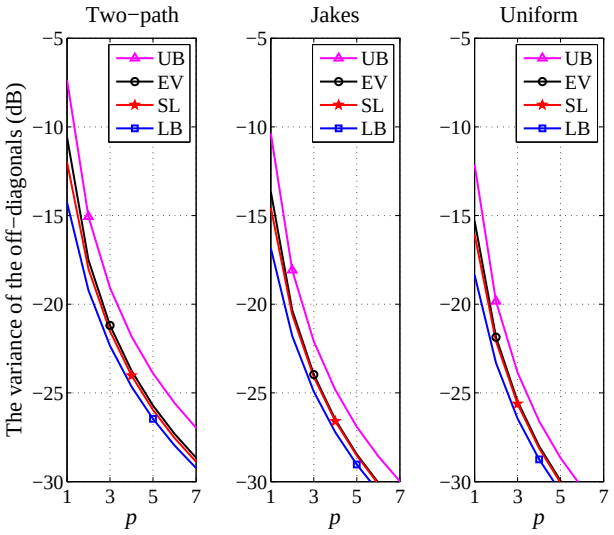

Fig. 1. Comparisons of the bounds, the simple lower bounds and the evaluations of the variances of the off-diagonal coefficients in channel matrix.

In Fig. 1, the tightness of the bounds in (17) and the simple lower bound in (23) are examined with the exact evaluation of the variances of the off-diagonal coefficients. We consider the OFDM systems with $N = 256$ subcarriers in the channel models listed in Table I of the normalized maximum Doppler frequency $f_D = 30\%$. The lower bounds (LB) are obviously closer to exact evaluations (EV) than the upper bounds (UB). Being tighter than the lower bounds (LB), the simple lower bounds (SL) are indeed very close to the exact evaluations (EV) even when the normalized maximum Doppler frequency is as high as 30%.

III. The Banded Approximations

A. The banded approximation errors

In this subsection, we derive the errors introduced with the manipulation of the banded approximation to a channel matrix for the OFDM systems. Specifically, manipulating a Qth banded approximation to a $N \times N$ channel matrix $\mathbf{H}$ results in the Qth banded channel matrix $\mathbf{H}_{(Q)} = \mathbf{H} \circ \mathbf{T}_{(Q)}$ where $\mathbf{T}_{(Q)}$ represents the $N \times N$ circulant matrix with all ones in the $2Q+1$ central diagonals, the $Q \times Q$ lower triangular matrix in the bottom-left corner and the $Q \times Q$ upper triangular matrix in the top-right corner, and all zeros else [15].

Manipulating a Qth banded approximation to the channel matrix $\mathbf{H}$ in (1), we obtain the OFDM system as

$$\mathbf{z} = \mathbf{H}_{(Q)}\mathbf{x} + \mathbf{n} + \epsilon \tag{24}$$

This article has been accepted for publication in a future issue of this journal, but has not been fully edited. Content may change prior to final publication. Citation information: DOI 10.1109/TVT.2014.2359233, IEEE Transactions on Vehicular Technology

where ϵ denotes the vector for the banded approximation errors of the variance

$$\sigma_B{}^2(Q) \equiv \frac{E\left\{\left\|\mathbf{H}_{(Q)}-\mathbf{H}\right\|^2\right\}}{E\left\{\left\|\mathbf{H}\right\|^2\right\}} = 2\sum_{p=Q+1}^{\frac{N}{2}-1}\sigma_F{}^2(p). \quad (25)$$

Using the bounds on $\sigma_F{}^2(p)$ in (17), we obtain a pair of upper and lower bounds as

$$\begin{aligned} &2\sum_{p=Q+1}^{\frac{N}{2}-1}\frac{\alpha_1(\pi f_D)^2-\frac{\alpha_2}{3}(\pi f_D)^4}{N^2\sin^2\left(\frac{\pi}{N}(p+f_D)\right)} \le \sigma_B{}^2(Q) \\ &\le 2\sum_{p=Q+1}^{\frac{N}{2}-1}\frac{\alpha_1(\pi f_D)^2}{N^2\sin^2\left(\frac{\pi}{N}(p-f_D)\right)},\ 0\le Q\le\tfrac{N}{2}-1. \end{aligned} \quad (26)$$

Considering the channel models of symmetric Doppler spectrum, we insert (22) into (25) and derive a tighter lower bound on the banded approximation errors as

$$\begin{aligned} \sigma_B{}^2(Q) &\ge 2\sum_{p=Q+1}^{\frac{N}{2}-1}\frac{\alpha_1(\pi f_D)^2-\frac{\alpha_2}{3}(\pi f_D)^4}{N^2\sin^2\left(\frac{\pi p}{N}\right)}, \\ &= 2\left(\sum_{p=1}^{\frac{N}{2}-1}\frac{1}{N^2\sin^2\left(\frac{\pi p}{N}\right)}-\sum_{p=1}^{Q}\frac{1}{N^2\sin^2\left(\frac{\pi p}{N}\right)}\right) \\ &\quad\times\left(\alpha_1(\pi f_D)^2-\frac{\alpha_2}{3}(\pi f_D)^4\right),\ 0\le Q\le\tfrac{N}{2}-1. \end{aligned} \quad (27)$$

The ICI power for the systems of finite subcarrier number has no significant difference from that for infinite [8], [23]. To resolve (27), we consider $N\to\infty$ and obtain

$$\begin{aligned} \lim_{N\to\infty}\sum_{p=1}^{\frac{N}{2}-1}\frac{1}{N^2\sin^2\left(\frac{\pi p}{N}\right)} &= \lim_{N\to\infty}\sum_{p=1}^{\frac{N}{2}-1}\frac{1}{N^2\left(\frac{\pi p}{N}\right)^2} \\ &= \pi^{-2}\sum_{p=1}^{\infty}p^{-2} = 1/6. \end{aligned} \quad (28)$$

TABLE II. The convergence and the approximation of $\sum_p \frac{1}{N^2\sin^2\left(\frac{\pi p}{N}\right)}$.

N	$\sum_{p=1}^{\frac{N}{2}-1}\frac{1}{N^2\sin^2\left(\frac{\pi p}{N}\right)}$	$\sum_{p=1}^{\frac{N}{2}-1}\frac{1}{(\pi p)^2}$	difference
64	0.1665	0.1635	0.0031
128	0.1666	0.1651	0.0016
256	0.1667	0.1659	0.0008
1024	0.1667	0.1665	0.0002
4096	0.1667	0.1667	0.0000
∞	1/6	1/6	0

In Table II, we examine the convergence and the approximation of $\sum_{p=1}^{\frac{N}{2}-1}N^{-2}\sin^{-2}\left(\frac{\pi p}{N}\right)$ with the numerical results for some candidate N. Assuming $N\ge 128$ and two-place approximations, we obtain

$$\sum_{p=1}^{\frac{N}{2}-1}\frac{1}{N^2\sin^2\left(\frac{\pi p}{N}\right)} = 1/6 \quad (29)$$

and

$$\sum_{p=1}^{Q}\frac{1}{N^2\sin^2\left(\frac{\pi p}{N}\right)} = \sum_{p=1}^{Q}\frac{1}{(\pi p)^2},\ 0\le Q\le\tfrac{N}{2}-1. \quad (30)$$

Inserting (29) and (30) into (27), we obtain a simple lower bound on the banded approximation errors for the OFDM systems in the channels of symmetric Doppler spectrum as

$$\sigma_B{}^2(Q) \ge \left(\frac{\pi^2}{3}-2\sum_{p=1}^{Q}\frac{1}{p^2}\right)\left(\alpha_1 f_D{}^2-\frac{\alpha_2}{3}\pi^2 f_D{}^4\right), \quad 0\le Q\le\tfrac{N}{2}-1. \quad (31)$$

Recalling (25) and (27), we note that the simple lower bound on the banded approximation errors in (31) are derived from the sum of the lower bounds on the variance of off-diagonal coefficients, and hence accumulates the errors of the lower bound on the variances of the off-diagonal coefficients from $p=Q+1$ to $p=\frac{N}{2}-1$. Based on the approximation of the 4th-order Taylor expansions, the accumulated errors are obtained as

$$\begin{aligned} \varepsilon_B(Q) &= 2\sum_{p=Q+1}^{\frac{N}{2}-1}\varepsilon_F(p) = 2\sum_{p=Q+1}^{\frac{N}{2}-1}\frac{1}{p^4}\left(3\alpha_2 f_D{}^4\right) \\ &= \left(\frac{\pi^4}{45}-2\sum_{p=1}^{Q}\frac{1}{p^4}\right)\left(3\alpha_2 f_D{}^4\right),\ 0\le Q\le\tfrac{N}{2}-1. \end{aligned} \quad (32)$$

Inserting $Q=0$ into (32), we obtain the total accumulated errors $\varepsilon_B(0)=\frac{\alpha_2}{15}(\pi f_D)^4$ equal to the difference between the lower bound of P_{ICI} in (12) and the lower bound of $\sigma_B{}^2(0)$ in (31). It can be easily obtained that $\varepsilon_B(Q) < 0.08\ \varepsilon_B(0)$ for $Q\ge 1$, and therefore the simple lower bound in (31) approximates $\sigma_B{}^2(Q)$ with negligible errors $\varepsilon_B(Q)$ for $1\le Q\le\frac{N}{2}-1$.

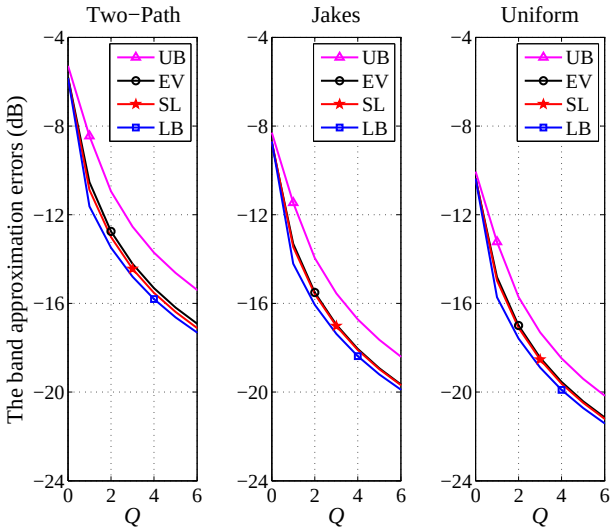

Fig. 2. Comparisons of the bounds, the simple lower bound and the evaluations of the banded approximation errors.

In Fig. 2, the tightness of the bounds in (26) and the simple lower bound in (31) are examined with the exact evaluation of the banded approximation errors. We consider the OFDM

This article has been accepted for publication in a future issue of this journal, but has not been fully edited. Content may change prior to final publication. Citation information: DOI 10.1109/TVT.2014.2359233, IEEE Transactions on Vehicular Technology

systems with $N = 256$ subcarriers in the channel models listed in Table I of the normalized maximum Doppler frequency $f_D = 30\%$. The bounds of P_{ICI} in (12) substitute for those of ${\sigma_B}^2(0)$ in (26) and (31) to eliminate the presence of the accumulated errors $\varepsilon_B(0)$. The relations among the upper bounds (UB), the exact evaluations (EV), the lower bound (LB) and the simple lower bound (SL) are similar to those in Fig. 1. Both the lower bound (LB) and the simple lower bound (SL) approach the exact evaluations (EV) in all of the instances.

B. The ICI mitigation with the banded equalizers

To evaluate the ICI power mitigated with the banded equalizers, we consider $g(Q) \equiv \frac{P_{ICI}}{{\sigma_B}^2(Q)}$ representing the ratio of the total ICI power to the residual ICI power in the Qth banded channel matrix $\mathbf{H}_{(Q)}$ in (24). Since $\varepsilon_B(0)$ is the only significant term in (32), we employ (31) to approximate ${\sigma_B}^2(Q)$, $1 \le Q \le \frac{N}{2} - 1$ and obtain

$$g(Q) = \frac{{\sigma_B}^2(0) + \varepsilon_B(0)}{{\sigma_B}^2(Q)} \ge \frac{{\sigma_B}^2(0)}{{\sigma_B}^2(Q)} = \frac{1}{\left(1 - \frac{6}{\pi^2}\sum_{p=1}^{Q}\frac{1}{p^2}\right)}, Q \ge 0. \tag{33}$$

In Fig. 3, we compare the ICI-mitigation gains $g(Q)$ in different conditions: 1) the prior universal lower bound (PLB) on $g(Q)$ previously derived in [8] (section III); 2) the simple universal lower bound (SLB) given in (33); 3) the exact evaluations of $g(Q)$ for the OFDM systems with $N = 256$ subcarriers in the specific channel models. The "U-10%" denotes the uniform Doppler spectrum of the normalized maximum Doppler frequency $f_D = 10\%$; "J-10%" denotes the Jakes Doppler spectrum of $f_D = 10\%$, and "T-10%" denotes the two-path Doppler spectrum of $f_D = 10\%$. The legends for those of the normalized maximum Doppler frequencies $f_D = 30\%$ and $f_D = 70\%$ are similarly inferred.

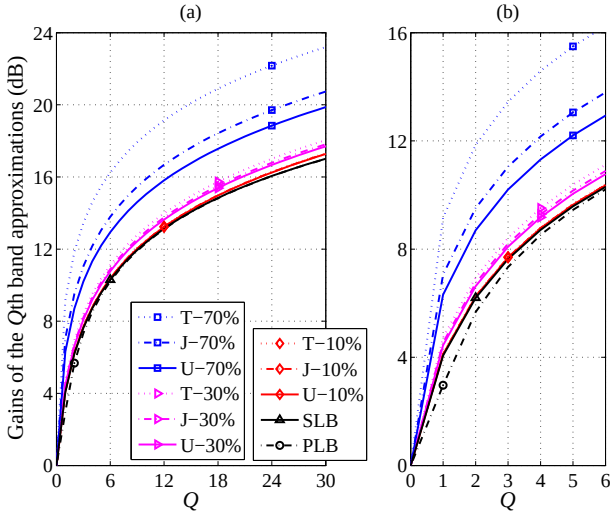

Fig. 3. The ICI-mitigation gains of the banded equalizers (a) a wide range of the band; (b) a close-up view for smaller bands.

As compared to the prior lower bound (PLB), the simple lower bound (SLB) in (33) is beneficial in tightness and simplicity. Several useful insights into the banded approximations are observed in Fig. 3. First, the 1st ($Q = 1$) banded equalizer mitigates the ICI power to –4 dB at least. Hence, more than 60% of the total ICI power comes from the pair of the 1st adjacent subcarriers. Similarly, the 2nd ($Q = 2$) banded equalizer decreases the ICI power to –6 dB at least. Hence, at least, accumulated 75% of the total ICI power comes from the 2nd neighboring subcarriers, and so forth. Second, the more total ICI power the systems suffer, the higher ratio the banded equalizers mitigate the ICI power. Third, the 2nd banded equalizers reduce the total ICI power to only –6 dB, and hence the bands selected in $Q \ge 2$ [15] is necessary in general application. Fourth, the increase of bands apparently returns diminishing gains of ICI mitigation for the system in the channel models listed in Table I. The rapid ascent of the gains ends after $Q = 6$, therefore, the efficient use of bands can be suggested to be in the range $2 \le Q \le 6$. Eventually, the banded equalizers with an efficient band mitigate the ICI less than 11 dB. In spite of a large band $Q = 30$ (hence computational complexity of the equalizers may dramatically increase), the ICI-mitigation gains are limited to 18 dB.

While the total ICI power can be known to the systems through well established methods, the banded approximation errors can be estimated without information of channel states. Upon ${\sigma_B}^2(Q) = \left(1 - \frac{6}{\pi^2}\sum_{p=1}^{Q}\frac{1}{p^2}\right){\sigma_B}^2(0)$, the banded approximation errors are overestimated by

$$ {\sigma_B}^2(Q) \approx \left(1 - \frac{6}{\pi^2}\sum_{p=1}^{Q}\frac{1}{p^2}\right)P_{ICI} \tag{34}$$

with an error $\varepsilon_g \equiv P_{ICI}/{\sigma_B}^2(0) \approx \left(\frac{\alpha_1}{3}{f_D}^2 - \frac{2\alpha_2}{45}\pi^2{f_D}^4\right) / \left(\frac{\alpha_1}{3}{f_D}^2 - \frac{\alpha_2}{9}\pi^2{f_D}^4\right)$. Considering the Jakes channels model with $f_D = 30\%$ as an example, we obtain $\varepsilon_g = 0.69$ dB which is negligible.

C. A generalized application

In this subsection, we propose a generalized application of the acquisition of the banded approximation errors for the MMSE banded equalizers previously proposed in [8], [9], [14]–[18]. As a common component, the linear MMSE estimation core was employed in the MMSE banded equalizers. Without loss of generality, we consider a simplified linear MMSE estimation core for the system in (24) as

$$\hat{\mathbf{x}_k} = {\mathbf{H}_k}^H\left(\mathbf{H}_k\mathbf{H}_k^H + \gamma^{-1}\mathbf{I}_{N_k}\right)^{-1}\mathbf{z}_k. \tag{35}$$

In the block linear MMSE banded equalizers [16]–[18], $\mathbf{x}_k$ denotes the data vector which is the central vector of $\mathbf{x}$ after removal of the guard bands [17]. Corresponding to $\mathbf{x}_k$, $\mathbf{H}_k$ and $\mathbf{z}_k$ denote the central block of $\mathbf{H}_{(Q)}$ and the central vector of $\mathbf{z}$, respectively. The N_k denotes the size of $\mathbf{H}_k$ and γ denotes the signal-to-interference-plus-noise ratio (SINR) of the systems. In the serial MMSE linear equalizers [8], [15], alternatively, $\mathbf{x}_k$ denotes the $2Q + 1$ sub-vector taken from $\mathbf{x}$. The central element of $\mathbf{x}_k$ maps to the kth element of $\mathbf{x}$. Corresponding to $\mathbf{x}_k$, $\mathbf{z}_k$ and $\mathbf{H}_k$ denotes the $(2Q+1)$ sub-vector and $(2Q+$

This article has been accepted for publication in a future issue of this journal, but has not been fully edited. Content may change prior to final publication. Citation information: DOI 10.1109/TVT.2014.2359233, IEEE Transactions on Vehicular Technology

$1)\times(2Q+1)$ sub-block of $\mathbf{H}_{(Q)}$, respectively. The N_k equals to $2Q+1$ and γ denotes SINR of the systems.

Thanks to the property of ICI power behaving as additive zero-mean Gaussian noise [26], [27], we handle ϵ in the systems in (24) as the Gaussian interference of the variance equal to ${\sigma_B}^2(Q)$. Hence, we obtain SINR in (35) as

$$\gamma = \left({\sigma_n}^2 + {\sigma_B}^2(Q)\right)^{-1} \tag{36}$$

where ${\sigma_n}^2$ denotes the variance of the Gaussian noise in the channels.

In next section, we examine the application with the BER performance for the block MMSE banded equalizers [17] and the block turbo MMSE banded equalizers [18], respectively.

IV. Simulation

In this section, we consider an OFDM system with $N = 256$ subcarriers, a CP of length equal to the maximum channel delay spreads $L = 8$ and QPSK modulation. The Rayleigh fading channels with Jakes Doppler spectrum and the exponential delay profile ${\sigma_t}^2(l) = e^{-0.3l}/\sum_{l=0}^{L-1} e^{-0.3l}$ for $l = 0,1,\cdots,L-1$ are employed to generate contiguous realizations for the time-varying channels. In all of the instances, we assume the perfect channel knowledge is available.

In the first set of simulations, we compute the ideal channel matrices $\mathbf{H}$ in (2) for individual symbol durations. With the statistics of the ideal channel matrices, we examine the variances of the off-diagonal coefficients in (23) and the banded approximation errors in (31), respectively.

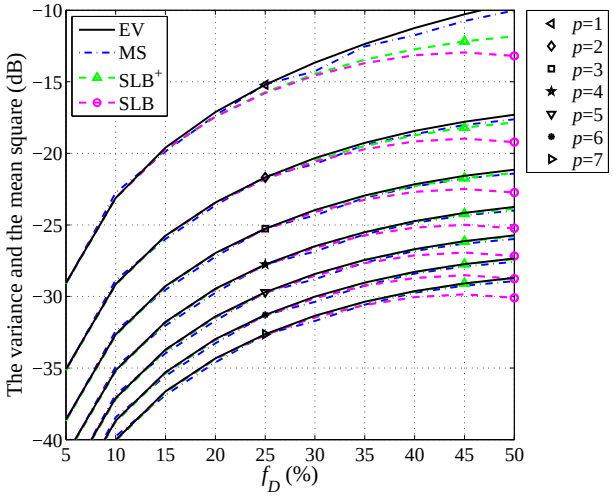

Fig. 4. Comparisons of the variances of the off-diagonal coefficients derived from the exact evaluations, the simple lower bounds and simulations.

Fig. 4 depicts the variances of the off-diagonal coefficients, ${\sigma_F}^2(p)$, with the mean squares (MS) of the coefficients of the same Doppler index (p) for $1 \le p \le 7$ in the ideal channel matrices. The variances ${\sigma_F}^2(p)$ are evaluated by (8), and approximated with both the simple lower bound (SLB) in (23) and the simple lower bound (SLB$^+$) enhanced in (42), respectively. As shown, the exact evaluation (EV) and the SLB$^+$ can precisely predict the mean squares (MS) of the pth off-diagonal coefficients, $p \ge 2$, through a wide range of f_D. The presence of the errors $\varepsilon_F(p)$ is apparent only in the curves for ${\sigma_F}^2(1)$ because $\varepsilon_F(p)$ decreases with $1/p^4$ as given in Appendix B. For $f_D \le 30\%$, the SLB is a good substitute for SLB$^+$, for the purpose of simplicity.

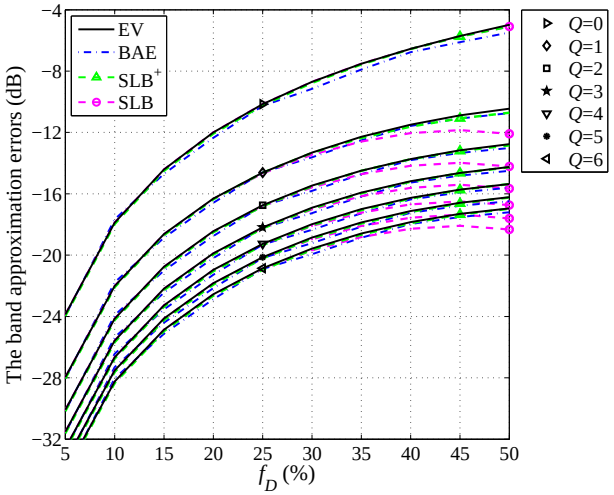

Fig. 5. Comparisons of the banded approximation errors derived from the exact evaluations, the simple lower bounds and simulations.

Fig. 5 illustrates the banded approximation errors versus the normalized maximum Doppler frequency for the bands in $0 \le Q \le 6$. Employing the ideal channel matrices, we derive the banded approximation errors (BAE) with ${\sigma_B}^2(Q) = E\{\|\mathbf{H}_{(Q)} - \mathbf{H}\|^2\}/E\{\|\mathbf{H}\|^2\}$. The exact evaluation (EV) of the banded approximation errors is derived as ${\sigma_B}^2(Q) = 2\sum_{p=Q+1}^{N/2-1} {\sigma_F}^2(p)$ where ${\sigma_F}^2(p)$ are evaluated with (8). The SLB is derived from (31), and the enhanced simple lower bound SLB$^+$ is derived from (43) for $1 \le Q \le 6$. For $Q = 0$, both of the SLB and the SLB$^+$ are derived from the lower bound of P_{ICI} in (12). As shown, the SLB approaches ${\sigma_B}^2(Q)$ with accuracy and simplicity for $f_D \le 30\%$ at the least, and the SLB$^+$ approaches ${\sigma_B}^2(Q)$ through the whole range of f_D. The most accumulated error $\varepsilon_B(0)$ is eliminated by substituting P_{ICI} in (12) for ${\sigma_B}^2(0)$. As a consequence, the accumulated errors $\varepsilon_B(Q)$, $0 \le Q \le 6$ can be seen to be insignificant. The curves of the banded approximation errors gradually become closer to each other with the increasing band Q. Therefore, the gains in ICI suppression diminish with the increasing bands, as those depicted in Fig. 3.

In the second set of simulations, we examine the application of the acquisition of the banded approximation errors with the BER performance of the block MMSE banded equalizers. The standard block MMSE banded equalizer in [17] and the block turbo MMSE banded equalizer [18] running 5 iterations are used in the tests. Seven instances of the block MMSE banded equalizers with the MMSE estimation core in (35) are considered respectively: 1) The block least square (LS) banded equalizer, i.e., inserting $\gamma^{-1} = 0$ into (35) to degrade the MMSE estimation to the LS estimation. 2) The standard block MMSE banded equalizer that ignores the banded approximation errors, i.e., $\gamma^{-1} = {\sigma_n}^2$. 3) The standard block MMSE

This article has been accepted for publication in a future issue of this journal, but has not been fully edited. Content may change prior to final publication. Citation information: DOI 10.1109/TVT.2014.2359233, IEEE Transactions on Vehicular Technology

banded equalizer that overestimates the banded approximation error to the total ICI power, i.e., $\gamma^{-1} = {\sigma_n}^2 + P_{ICI}$. 4) The standard block MMSE banded equalizer that employs the SINR given in (36). 5) The block turbo MMSE banded equalizer that ignores the banded approximation errors. 6) The block turbo MMSE banded equalizer that overestimates the banded approximation error to the total ICI power. 7) The block turbo MMSE banded equalizer that employs the SINR given in (36).

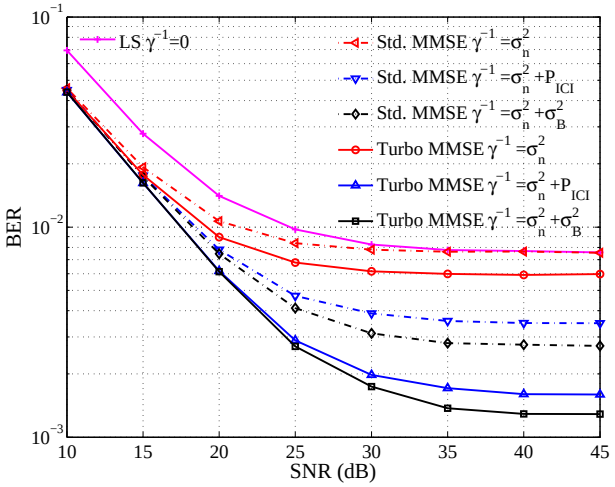

Fig. 6. The BER performance of the instances of the block MMSE banded equalizers with the 2nd banded channel matrix.

In Fig. 6, we examine the BER performance of the seven instances of the block MMSE banded equalizers manipulating a $Q = 2$ banded approximation to the ideal channel matrix. The normalized maximum Doppler frequency of the LTV channels is set to $f_D = 15\%$. On the comparisons with the error floors, Fig. 6 depicts both of the standard block MMSE banded equalizers and the block turbo MMSE banded equalizers are suboptimal if the banded approximation errors are ignored to zeros. The benefits from inputs of the banded approximation errors (or the total ICI power) to the MMSE estimation core are twofold: the lower error floors to the standard block MMSE banded equalizers and the enhanced gains from the iterations of the block turbo MMSE banded equalizers. Provided the total ICI power P_{ICI} is known with some methods, we easily estimate the banded approximation errors with (34) to improve the BER performance of the block MMSE banded equalizers.

Fig. 7 depicts the BER performance of the seven instances of the block MMSE banded equalizers which employ a $Q = 6$ banded channel matrix. As compared to Fig. 6, the benefits from inputs of the banded approximation errors to the MMSE estimation core become more significant in spite of the smaller amount of the banded approximation errors. As a consequence, the knowledge of the banded approximation errors are essential to the block (turbo) MMSE banded equalizers seeking for precise detections with large-tap (i.e., a big Q) equalizations.

Fig. 8 depicts the error floors of the seven instances of the block MMSE banded equalizers through the bands in $0 \leq Q \leq 24$ for the high-mobility channels ($f_D = 10\%$) and the very-high-mobility channel ($f_D = 20\%$) [11], respectively. Inserting a sufficiently low variance of the Gaussian noise ${\sigma_n}^2 = -55$ dB, we derive the error floors for the seven instances. We do not plot for the block LS banded equalizer because it shares the same error floors with the standard block MMSE banded equalizer that sets the banded approximation errors to zeros. As shown, the efficient bands selected in $2 \leq Q \leq 6$ reach appropriate tradeoffs between the BER performance and the computational complexity for the block (turbo) MMSE banded equalizers in the channels of different levels of mobilities. By comprehensive comparisons in Fig. 8, the block MMSE banded equalizer, with more powerful detections (e.g., with iterations or/and large-tap equalizations) and with the channels of the higher mobility, gains more error rate improvements from the acquisition of the banded

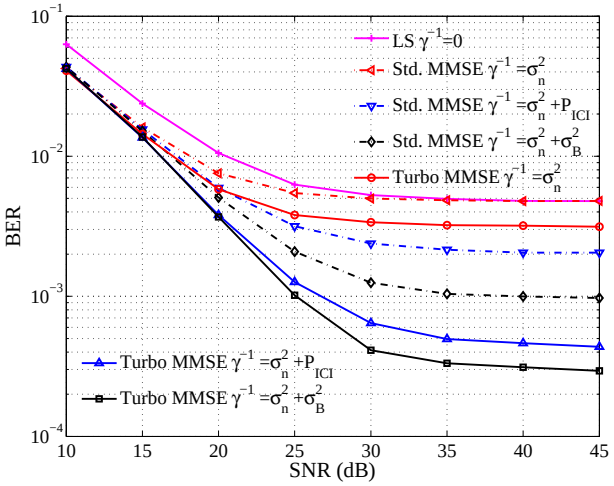

Fig. 7. The BER performance of the instances of the block MMSE banded equalizers with the 6th banded channel matrix.

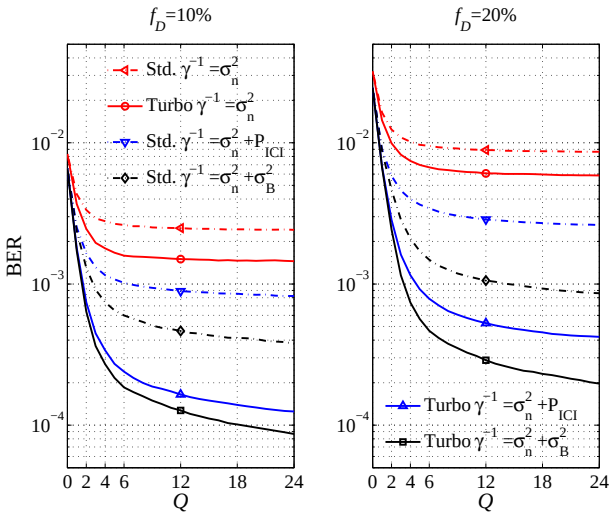

Fig. 8. The error floors of the block MMSE banded equalizers in the channels of high mobility and very high mobility, respectively.

This article has been accepted for publication in a future issue of this journal, but has not been fully edited. Content may change prior to final publication. Citation information: DOI 10.1109/TVT.2014.2359233, IEEE Transactions on Vehicular Technology

approximation errors.

V. Conclusion

This paper investigates the banded approximation of the frequency-domain channel matrix of the OFDM systems in time-varying channels. We derive the simple lower bounds on the variance of the coefficients in the channel matrix, the banded approximation errors and the ICI-mitigation gains of the banded equalizers, respectively. We provide perspectives inside the channel matrix, measure the side effects to manipulate the banded approximation on the channel matrix, and herewith provide a guideline to select an efficient band for the banded equalizers. By using the variances of the banded approximation errors in the MMSE estimation, both the standard block MMSE banded equalizers and the block turbo MMSE banded equalizers generate significantly lower error floors than those ignoring the presence of the banded approximation errors.

Appendix A

Letting α denote $\frac{\pi p}{N}$ and β denote $\frac{\pi f}{N}$, we aim to prove $\sin^{-2}(\alpha-\beta)+\sin^{-2}(\alpha+\beta)\geq 2\sin^{-2}\alpha$ with the condition $0\leq\beta\leq\alpha<\frac{\pi}{2}$. Considering

$$\begin{aligned}&\frac{1}{\sin^2(\alpha-\beta)}+\frac{1}{\sin^2(\alpha+\beta)}\\&=\frac{2\left(\left(\sin\alpha\cos\beta\right)^2+\left(\sin\beta\cos\alpha\right)^2\right)}{\left(\left(\sin\alpha\cos\beta\right)^2-\left(\sin\beta\cos\alpha\right)^2\right)^2}\end{aligned}\tag{37}$$

and $0\leq\left(\sin\beta\cos\alpha\right)^2<\left(\sin\alpha\cos\beta\right)^2$, we obtain

$$\frac{1}{\sin^2(\alpha-\beta)}+\frac{1}{\sin^2(\alpha+\beta)}\geq\frac{2}{\sin^2\alpha\cos^2\beta}\geq\frac{2}{\sin^2\alpha}\tag{38}$$

by dropping $\left(\sin\beta\cos\alpha\right)^2$ from the numerator and the denominator in (37).

Appendix B

Assuming the channel model is with symmetric Doppler spectrum, we intend to approximate the difference between the simple lower bound in (23) and the exact valuation of (8). Considering $N\rightarrow\infty$, we obtain

$$\begin{aligned}&\frac{1}{N^2}\left(\sin^{-2}\left(\frac{\pi}{N}\left(p-f\right)\right)+\sin^{-2}\left(\frac{\pi}{N}\left(p+f\right)\right)\right)\\&=\pi^{-2}\left(p-f\right)^{-2}+\pi^{-2}(p+f)^{-2}\\&=\frac{2\left(p^2+f^2\right)}{\pi^2\left(p^2-f^2\right)^2}=2\left(\frac{1}{\pi^2p^2}+\frac{3f^2}{\pi^2p^4}+\cdots\right).\end{aligned}\tag{39}$$

Inserting (39) into (20), we derive

$$\begin{aligned}{\sigma_F}^2(p)&=\int_{-f_D}^{f_D}s\left(f\right)\sin^2\left(\pi f\right)\left(\frac{1}{\pi^2p^2}+\frac{3f^2}{\pi^2p^4}+\cdots\right)df\\&=\int_{-f_D}^{f_D}s\left(f\right)\left(\pi^2f^2-\frac{1}{3}\pi^4f^4+\cdots\right)\\&\qquad\times\left(\frac{1}{\pi^2p^2}+\frac{3f^2}{\pi^2p^4}+\cdots\right)df.\end{aligned}\tag{40}$$

In the approximations of the 4th-order Taylor expansions, we convert (40) to

$${\sigma_F}^2(p)=\frac{1}{p^2}\left(\alpha_1{f_D}^2-\frac{\alpha_2}{3}\pi^2{f_D}^4\right)+\frac{3\alpha_2{f_D}^4}{p^4}.\tag{41}$$

Consequently, the difference between ${\sigma_F}^2(p)$ and its simple lower bound in (23) is derived as $\varepsilon_F(p)=\frac{3\alpha_2{f_D}^4}{p^4}$.

Appendix C

Here we consider the systems with relatively high Doppler frequencies where the approximations by the 4th-order Taylor expansions are insufficient. By using the 8th-order Taylor expansions, we improve (23) to

$${\sigma_F}^2(p)\geq\frac{1}{p^2}\left(\alpha_1{f_D}^2-\frac{\alpha_2}{3}\pi^2{f_D}^4+\frac{2\alpha_3}{45}\pi^4{f_D}^6-\frac{\alpha_4}{315}\pi^6{f_D}^8\right),\tag{42}$$

and (31) to

$$\begin{aligned}{\sigma_B}^2(Q)\geq&\left(\frac{\pi^2}{3}-2\sum_{p=1}^{Q}\frac{1}{p^2}\right)\\&\times\left(\alpha_1{f_D}^2-\frac{\alpha_2}{3}\pi^2{f_D}^4+\frac{2\alpha_3}{45}\pi^4{f_D}^6-\frac{\alpha_4}{315}\pi^6{f_D}^8\right),\end{aligned}\tag{43}$$

where α_3 and α_4 for the channel models of interest are supplemented in Table III.

TABLE III. The α_3 and α_4 for the channel models of interest.

Models	Two-path	Jakes	Uniform
α_3, α_4	1, 1	$\frac{5}{16}$, $\frac{35}{128}$	$\frac{1}{7}$, $\frac{1}{9}$

References

[1] Z. Wang and G. Giannakis, "Wireless multicarrier communications," *IEEE Signal Processing Magazine*, vol. 17, no. 3, pp. 29 –48, May 2000.

[2] T. Wang, J. Proakis, E. Masry, and J. Zeidler, "Performance degradation of OFDM systems due to Doppler spreading," *IEEE Transactions on Wireless Communications*, vol. 5, no. 6, pp. 1422 –1432, June 2006.

[3] W.-G. Song and J.-T. Lim, "Pilot-symbol aided channel estimation for OFDM with fast fading channels," *IEEE Transactions on Broadcasting*, vol. 49, no. 4, pp. 398 –402, Dec. 2003.

[4] Y. Mostofi and D. Cox, "ICI mitigation for pilot-aided OFDM mobile systems," *IEEE Transactions on Wireless Communications*, vol. 4, no. 2, pp. 765 – 774, March 2005.

[5] C. Shin, J. Andrews, and E. Powers, "An efficient design of doubly selective channel estimation for OFDM systems," *IEEE Transactions on Wireless Communications*, vol. 6, no. 10, pp. 3790 –3802, Oct. 2007.

[6] S. U. Hwang, J. H. Lee, and J. Seo, "Low complexity iterative ICI cancellation and equalization for OFDM systems over doubly selective channels," *IEEE Transactions on Broadcasting*, vol. 55, no. 1, pp. 132 –139, March 2009.

[7] H. Hijazi and L. Ros, "Polynomial estimation of time-varying multipath gains with intercarrier interference mitigation in OFDM systems," *IEEE Transactions on Vehicular Technology*, vol. 58, no. 1, pp. 140 –151, Jan. 2009.

[8] X. Cai and G. Giannakis, "Bounding performance and suppressing intercarrier interference in wireless mobile OFDM," *IEEE Transactions on Communications*, vol. 51, no. 12, pp. 2047 –2056, Dec. 2003.

[9] A. Gorokhov and J.-P. Linnartz, "Robust OFDM receivers for dispersive time-varying channels: equalization and channel acquisition," *IEEE Transactions on Communications*, vol. 52, no. 4, pp. 572 –583, April 2004.

[10] S. Lu and N. Al-Dhahir, "Coherent and differential ICI cancellation for mobile OFDM with application to DVB-H," *IEEE Transactions on Wireless Communications*, vol. 7, no. 11, pp. 4110 –4116, November 2008.

This article has been accepted for publication in a future issue of this journal, but has not been fully edited. Content may change prior to final publication. Citation information: DOI 10.1109/TVT.2014.2359233, IEEE Transactions on Vehicular Technology

[11] T. Al-Naffouri, K. Islam, N. Al-Dhahir, and S. Lu, "A model reduction approach for OFDM channel estimation under high mobility conditions," *IEEE Transactions on Signal Processing*, vol. 58, no. 4, pp. 2181 –2193, April 2010.
[12] Z. Tang, R. Cannizzaro, G. Leus, and P. Banelli, "Pilot-assisted time-varying channel estimation for OFDM systems," *IEEE Transactions on Signal Processing*, vol. 55, no. 5, pp. 2226 –2238, May 2007.
[13] X. Huang and H.-C. Wu, "Robust and efficient intercarrier interference mitigation for OFDM systems in time-varying fading channels," *IEEE Transactions on Vehicular Technology*, vol. 56, no. 5, pp. 2517 –2528, Sept. 2007.
[14] W. G. Jeon, K. H. Chang, and Y. S. Cho, "An equalization technique for orthogonal frequency-division multiplexing systems in time-variant multipath channels," *IEEE Transactions on Communications*, vol. 47, no. 1, pp. 27 –32, Jan 1999.
[15] P. Schniter, "Low-complexity equalization of OFDM in doubly selective channels," *IEEE Transactions on Signal Processing*, vol. 52, no. 4, pp. 1002 –1011, April 2004.
[16] L. Rugini, P. Banelli, and G. Leus, "Low-complexity banded equalizers for OFDM systems in Doppler spread channels," *EURASIP Journal on Applied Signal Processing*, vol. 2006, pp. 1 –13, 2007.
[17] ——, "Simple equalization of time-varying channels for OFDM," *IEEE Communications Letters*, vol. 9, no. 7, pp. 619 –621, July 2005.
[18] K. Fang, L. Rugini, and G. Leus, "Low-complexity block turbo equalization for OFDM systems in time-varying channels," *IEEE Transactions on Signal Processing*, vol. 56, no. 11, pp. 5555 –5566, Nov. 2008.
[19] A. Molisch, M. Toeltsch, and S. Vermani, "Iterative methods for cancellation of intercarrier interference in OFDM systems," *IEEE Transactions on Vehicular Technology*, vol. 56, no. 4, pp. 2158 –2167, July 2007.
[20] G. Liu, S. Zhidkov, H. Li, L. Zeng, and Z. Wang, "Low-complexity iterative equalization for symbol-reconstruction-based OFDM receivers over doubly selective channels," *IEEE Transactions on Broadcasting*, vol. 58, no. 3, pp. 390–400, 2012.
[21] K. Kwak, S. Lee, H. Min, S. Choi, and D. Hong, "New OFDM channel estimation with dual-ICI cancellation in highly mobile channel," *IEEE Transactions on Wireless Communications*, vol. 9, no. 10, pp. 3155 –3165, Oct. 2010.
[22] K. Islam, T. Al-Naffouri, and N. Al-Dhahir, "On optimum pilot design for comb-type OFDM transmission over doubly-selective channels," *IEEE Transactions on Communications*, vol. 59, no. 4, pp. 930 –935, April 2011.
[23] Y. Li and J. Cimini, L.J., "Bounds on the interchannel interference of OFDM in time-varying impairments," *IEEE Transactions on Communications*, vol. 49, no. 3, pp. 401 –404, Mar 2001.
[24] J.-C. Lin, "Coarse frequency-offset acquisition via subcarrier differential detection for OFDM communications," *IEEE Transactions on Communications*, vol. 54, no. 8, pp. 1415–1426, Aug 2006.
[25] ——, "A frequency offset estimation technique based on frequency error characterization for OFDM communications on multipath fading channels," *IEEE Transactions on Vehicular Technology*, vol. 56, no. 3, pp. 1209–1222, May 2007.
[26] P. Robertson and S. Kaiser, "The effects of Doppler spreads in OFDM(A) mobile radio systems," in *IEEE Vehicular Technology Conference 50th*, vol. 1, 1999, pp. 329 –333 vol.1.
[27] M. Russell and G. Stuber, "Interchannel interference analysis of OFDM in a mobile environment," in *IEEE Vehicular Technology Conference 45th*, vol. 2, Jul 1995, pp. 820 –824 vol.2.

Ting-Li Liu received the M.S. degree in computer science from the National Chiao Tung University, Hsinchu, Taiwan, R.O.C., in 2006 and the Ph.D. degree in electrical engineering from the National Taiwan University, Taipei, Taiwan, R.O.C., in 2014. His research interests are in the areas of signal processing and mobile communications.

Wei-Ho Chung received the B.Sc. and M.Sc. degrees in Electrical Engineering from the National Taiwan University, Taipei, Taiwan, in 2000 and 2002, respectively, and the Ph.D. degree in Electrical Engineering from the University of California, Los Angeles, in 2009. From 2002 to 2005, he was a system engineer at ChungHwa Telecommunications Company, where he worked on data networks. In 2008, he worked on CDMA systems at Qualcomm, Inc., San Diego, CA. His research interests include communications, signal processing, and networks.

Dr. Chung received the Taiwan Merit Scholarship from 2005 to 2009 and the Best Paper Award in IEEE WCNC 2012, and has published over 40 refereed journal articles and over 50 refereed conference papers. Since January 2010, Dr. Chung has been a tenure-track assistant research fellow, and promoted to the rank of associate research fellow in January 2014. He leads the Wireless Communications Lab in the Research Center for Information Technology Innovation, Academia Sinica, Taiwan.

Shih-Yi Yuan received his Ph.D. degree in electrical engineering from National Taiwan University (NTU) in 1997. He has served as Technical committee Member in several IEEE-sponsored conferences for past 10 years and conducted several government projects with the Bureau of Standards, Metrology & Inspection, Ministry of Economic Affairs, Republic of China. He is now an associate professor at the Department of Communication Engineering and the section chief of planning of IC-EMC center, Feng Chia University. His research interests include signal process, embedded software design, and software solution for EM-aware compiler design.

Sy-Yen Kuo is the Dean of College of Electrical Engineering and Computer Science and a Distinguished Professor at the Department of Electrical Engineering, National Taiwan University(NTU), Taipei, Taiwan and was the Chairman at the same department from 2001 to 2004. He took a leave from NTU and served as a Chair Professor and Dean of the College of Electrical Engineering and Computer Science, National Taiwan University of Science and Technology from 2006 to 2009. He received the BS (1979) in Electrical Engineering from National Taiwan University, the MS (1982) in Electrical & Computer Engineering from the University of California at Santa Barbara, and the PhD (1987) in Computer Science from the University of Illinois at Urbana-Champaign. He spent his sabbatical years as a Visiting Professor at the Department of Computing, Hong Kong Polytechnic University from 2011-2012 and at the Computer Science and Engineering Department, the Chinese University of Hong Kong from 2004-2005, and as a visiting researcher at AT&T Labs-Research, New Jersey from 1999 to 2000, respectively. He was the Chairman of the Department of Computer Science and Information Engineering, National Dong Hwa University, Taiwan from 1995 to 1998, a faculty member in the Department of Electrical and Computer Engineering at the University of Arizona from 1988 to 1991, and an engineer at Fairchild Semiconductor and Silvar-Lisco, both in California, from 1982 to 1984. In 1989, he also worked as a summer faculty fellow at Jet Propulsion Laboratory of California Institute of Technology. His current research interests include dependable systems and networks, mobile computing, cloud computing, and quantum computing and communications.

Professor Kuo is an IEEE Fellow. He has published more than 390 papers in journals and conferences, and also holds 13 US patents, 9 Taiwan patents, and several other patents. He received the Distinguished Research Award 3 times consecutively and the Distinguished Research Fellow from the National Science Council, Taiwan. He was also a recipient of the Best Paper Award in the 1996 International Symposium on Software Reliability Engineering, the Best Paper Award in the simulation and test category at the 1986 IEEE/ACM Design Automation Conference(DAC), the National Science Foundation's Research Initiation Award in 1989, and the IEEE/ACM Design Automation Scholarship in 1990 and 1991.